Inflammopharmacology (2022) 30:173–184
https://doi.org/10.1007/s10787-021-00911-x

Inflammopharmacology

ORIGINAL ARTICLE

Anti-inflammatory and anti-COVID-19 effect of a novel polyherbal formulation (Imusil) via modulating oxidative stress, inflammatory mediators and cytokine storm

M. Ratheesh[1] · Sujatha Sunil[2] · S. Sheethal[1] · Svenia P. Jose[1] · S. Sandya[3] · Oriparambil Sivaraman Nirmal Ghosh[4] · Sony Rajan[1] · Tariq Jagmag[5] · Jayesh Tilwani[5]

Received: 26 September 2021 / Accepted: 6 December 2021 / Published online: 25 January 2022

Abstract

In the current scenario, most countries are affected by COVID-19, a pandemic caused by the severe acute respiratory syndrome coronavirus 2 (SARS-CoV-2) that has a massive impact on human health. Previous studies showed that some traditionally used medicinal herbs and their combinations showed synergistic anti-viral and anti-inflammatory activity against SARS-CoV-2 type infections. Therefore, the goal of this study is to demonstrate the anti-viral and anti-inflammatory effects of a novel polyherbal formulation, hereinafter referred to as Imusil, on Vero E6 cell lines and Raw 264.7 murine macrophage cells respectively. The Imusil was subjected to identify its chemical characterisations such as UV–Visible spectrum profile, Fourier transform infrared spectroscopy (FT-IR) and gas chromatography–mass spectroscopic (GC–MS) analysis. FT-IR analysis of Imusil peak values with various functional compounds such as alcohol, esters, aliphatic and carboxylic acids. GC–MS analysis of compounds with totally 87 compounds major chemical compounds were identified, such as 3-(Octanoyloxy) propane-1,2-diyl bis(decanoate), Succinic acid, 2-methylhex-3-yl 2,2,2-trifluoroethyl ester, Neophytadiene, 3,5,9-Trioxa-4-phosphaheneicosan-1-aminium, 4-hydroxy-*N*,*N*,*N*-trimethyl-10-oxo-7-[(1-oxododecyl)oxy]-, hydroxide, inner salt, 4-oxide, (R)-. The anti-viral activity of Imusil against SARS-CoV-2 was assessed using plaque reduction assay and anti-inflammatory study was conducted on lipopolysaccharide (LPS)-induced RAW 264.7 cells. The results obtained from the study reveal that Imusil significantly inhibited SARS-CoV-2 replication in Vero E6 cells and the production of inflammatory mediator's cyclooxygenase-2 and pro-inflammatory cytokines like tumour necrosis factor-α and interleukin- 6 were significantly reduced, along with thwarting the significant oxidative stress by preventing the expression of NOX-2 thereby inhibiting the reactive oxygen species formation. Hence, considering the current study as a novel strategy for mediating the COVID-19 associated aliments, inceptive scientific evidence of Imusil promises its potential therapeutic implications against COVID-19 and inflammatory conditions.

Keywords Inflammation · Imusil · Oxidative stress · NOX-2 · Pro-inflammatory cytokines · COVID-19

✉ M. Ratheesh
sivatheertha@gmail.com

1 Department of Biochemistry, St. Thomas College, Palai, Kottayam 686574, Kerala, India

2 Vector Borne Disease Group, International Centre for Genetic Engineering and Biotechnology, New Delhi, India

3 Inorganic and Physical Chemistry, Indian Institute of Science, Bangalore, Karnataka, India

4 Advanced Research Laboratory, Department Research Wing, DHME, Department of AYUSH, Thiruvananthapuram, Kerala, India

5 Glowderma Lab Pvt. Ltd, Mumbai, India

Introduction

The global pandemic COVID-19 caused by the SARS CoV-2 virus possesses a wide spectrum of pathological severity, ranging from asymptomatic to severe acute respiratory distress syndrome (ARDS) leading to the death of the individual. The severity of the disease is based on individual's health, age, obesity condition and morbidities like hypertension, diabetes etc. (Wolff et al. 2021). The chronic symptomatic conditions of COVID-19 like ARDS, acute cardiac complications, multiple organ dysfunction etc. are driven by an immunological stress response (García 2020). The barricades of the Innate immune system are the first to encounter

the virus and recognise pathogen associated molecular patterns (PAMPS) by pathogen recognition receptors (PRR) like NOD like receptors (NLR), Toll like receptors (TLR), angiotensin receptors etc. (Ky and Mann 2020; South et al. 2020). These in turn activate the production of transcription factors, nuclear factor κB (NF-κB) and activating protein 1 (AP-1) leading to the initiation of inflammatory pathways. Inflammatory responses are bring about by dendritic cell maturation and macrophage activation. As a result, it leads to the stimulation of T helper cells and occur an anomalous release of pro-inflammatory cytokines (IL-6, IL-1β and TNF) known as cytokine storm leads to hyper- inflammation (Lampropoulou et al. 2016).Apart from the inflammatory response, immune cells also induce the production of large amounts of free radicals at the site of viral replication, leading to oxidative stress (Ivanov et al. 2017). The mechanism of ROS production and oxidative stress during COVID-19 is explained hereafter. SARS CoV2 viral spike protein binds to angiotensin converting enzyme 2 (ACE2). ACE2 have other functions like balancing the angiotensin II (ATII) peptide hormone level in the blood. The proteolytic activity of ACE2 to cleave ATII is reduced during SARS CoV-2 infection because of the binding of the viruses to ACE2. This in turn raises the amount of ATII in the blood. AT1R acts as the receptor of ATII in endothelial cells, which further activates the MAP-kinase axis, protein kinase C, as well as NF-κB resulting in activation of NOX2, expression of cytokines and cyclooxygenase 2 (COX2). Endothelial NOX2 activation leads to the production of excessive reactive oxygen species (ROS) (Forrester et al. 2018). ROS production gives positive feedback to AT1R downstream signalling (Griendling et al. 1994). Thus, formed ROS further stimulates the formation of mitochondrial ROS (mtROS) and acts as fuel for the activation of further NOX2 in the endothelium leading to oxidative stress and endothelial damage (Chernyak et al. 2020). The overproduction of reactive oxygen species (ROS) and reactive nitrogen species (RNS) in the body is due to the failure of the antioxidant defence system to balance free radical scavenging and production. This may lead to oxidisation of biomolecules like DNA, RNA and proteins and alter the structure of proteins to a modified form, leading to signalling cascades of further inflammatory responses. This in turn prompts cell death and the ultimate result is organ damage (Mathern and Heeger 2015; Park et al. 2015). These types of damage associated with ROS production and oxidative stress play a vital role in the pathogenesis of COVID-19 (Varga et al. 2020).

Treatment methods for this type of viral disease often involve steroidal or non-steroidal drugs. The efficiency of these drugs to treat multiple aspects of the diseased conditions is yet to be understood. The need of therapeutics with anti-inflammatory, antioxidant, and immunomodulatory effects and anti-viral efficacy is increasing. Many biologically active compounds of plant origin have potent pharmacological efficacy. The role of natural products in combinatorial drug therapy and their synergistic therapeutical potential have recently been explored more by researchers.

Picrorhiza kurroa, a medicinal herb used in the Ayurvedic system of medicine is rich in chemical components with huge pharmacological benefits like immunomodulatory, anti-allergic, anti-anaphylatic, antioxidant and anti-neoplastic activities (Bhandari et al. 2008; Rajkumar et al. 2011). One of the major components of *Picrorhiza kurroa* is known as Apocyanin which possess miraculous health benefit like suppression of the production of reactive oxygen species by inhibiting NADPH oxidase and NADH oxidase (NOX) and Pro-inflammatory cytokines like IL-2, TNF-α, IFN-γ (Nam et al. 2014). Tinospora cordifolia is another herb that possesses a beneficial role in the treatment of viral diseases. Molecular docking studies revealed that Tinospora cordifolia can be made as a drug for SARS Cov2 due to its anti-viral efficacy of phytochemicals like berberine, β-sitosterol, octacosanol, tetrahydropalmatine, choline (Krupanidhi et al. 2020). The Anti-inflammatory and antioxidant activities of Tinospora underline its other beneficial pharmacological activities (Shwetha et al. 2016). *Emblica officianalis,* commonly called Indian gooseberry, is the richest source of vitamin C and is being used in traditional systems of medicine like Ayurveda and Siddha. Surplus amounts of low molecular weight hydrolysable tannins like emblicanin-A, emblicanin-B, Punigluconin and pedunculagin provide protection against oxygen free radicals. Thus, *Emblica officianalis* is a potent antioxidant, anti-inflammatory agent, cardio protective agent, anti-cancerous and immunomodulatory agent (Chowdhury 2020).

The role of a combinatorial drug with different pharmacological as well as therapeutical properties in treating COVID-19 via inflammatory and oxidative stress related pathways is yet to be elucidated. Therefore, in the current scenario, we investigated the anti- inflammatory and anti-COVID-19 effects of a polyherbal formulation of *Picrorhiza kurroa, Tinospora cordifolia and Emblica officianalis,* (hereinafter referred to as Imusil).

Materials and methods

Chemicals

All the chemicals and solvents are of analytical grade, obtained and used in the same condition. 3-(4,5-dimethylthiazol-2-yl)-2,5-diphenyl-tetrazolium bromide (MTT), Dulbecco's modified Eagle's medium (DMEM), foetal bovine serum (FBS), Penicillin–streptomycin (Sigma, St. Louis, MO, USA), ELISA kits for detecting TNF-α and IL-6 (R&D Systems, Inc., USA),

COX-2 Kit was obtained from Cayman Chemical Company, Antibodies specific for NOX-2 and glyceraldehydes 3-phosphate dehydrogenase (GADPH) (Santa Cruz Biotechnology, Inc., Santa Cruz, CA, USA).

Preparation of Imusil

Imusil contain 200 mg of extract of *Picrorhiza kurroa* (Kutki), 60 mg of extract of *Tinospora cordifolia* (Guduchi) and 60 mg of extract of *Emblica officinalis* (Gooseberry).

Characterisation of Imusil

UV–VIS spectrum analysis

The Imusil concentration was made as 1 mg/mL in hexane solvent. The Imusil was scanned at wavelength ranging from 200 to 1100 nm using Analytik jena model Specord 600 using deuterium and halogen lamp. Spectrophotometer and the characteristic peaks were detected. The peak values of the UV–VIS were recorded.

FT-IR analysis

To characterise the functional group present in Imusil Thermofisher Scientific's Fourier Transform Infrared spectroscopy model Nicolet iS50 FT-IR operating in transmission mode at a resolution of 4 cm^{-1} used. Imusil was ground into fine powder using agate mortar and FT-IR spectrometer in the region 4000–400 cm^{-1} by employing standard KBr pellet technique. 64 scans were single averaged to reduce the noise. The powdered sample of the pellet was loaded in FT-IR spectroscopy.

GC–MS analysis

The chemical constituents present in the Imusil was identified using Gas chromatography and mass spectrometry(GC–MS) by Agilent 7890A GC system, 5975C MS system with the column of dimensions 30 m × 250 µm × 0.25 µm. The initial temperature was 40 °C with a hold time of 2 min. The temperature was raised to 270 °C with a rate of 10 °C/min with a hold to time of 5 min. 1 µL of sample injected and the total run time was 37 min. The mass spectra of unknown peaks obtained from GC–MS were compared with the standard stored in GC–MS NIST library to identify the various chemical compounds present in the Imusil.

Experimental procedures: in vitro cell line culture

Vero E6 cell line culture

Vero E6 African green monkey kidney epithelial cells were used for the anti-viral study. The cells were maintained in DMEM containing 10% inactivated FBS in an incubator at 37 °C, 5% CO_2 and 75% Humidity. The concentration of FBS was reduced to 2% for the cytotoxicity and anti-viral assay.

MTT assay for cytotoxicity using Vero E6 cells.

The cytotoxic activity of Imusil on Vero E6 cells was determined by the MTT (3-(4, 5-dimethyl thiazol-2yl)-2, 5-diphenyl tetrazolium bromide) assay. Monolayer of Vero cells were plated in 96-well plate and incubated overnight for 18 h followed by the treatment with serially diluted Imusil along with negative control (media containing 0.1% DMSO) which was incubated for 48 h and 72 h. For the MTT assay, the medium from the wells was removed and each well was treated with 10 µL of MTT reagent (5 mg/mL). The plate was incubated for 4 h at 37 °C in a 5% CO_2 incubator for cytotoxicity. After incubation, 150 µL of DMSO (solublizing reagent) was added to each well and mixed well by micropipette and left for 45 s. The presence of viable cells was visualized by the development of a purple colour due to the formation of formazan crystals. The absorbance was measured at 595 nm using a microplate reader.

Antiviral activity of Imusil against SARS-CoV-2 in Vero E6 cell line

Briefly, 10,000 cells per well were seeded in a 96-well plate and incubated overnight as mentioned before. After the incubation, the highest non-cytotoxic concentration of Imusil in 100 µL of medium containing 2% FBS along with SARS-CoV-2 (MOI = 0.1) was added to each well and incubated at 37 °C and 5% CO_2. The supernatant was collected after 24 h and 48 h of incubation and the virus titre was estimated using plaque assay (Baer and Kehn-Hal 2014).

Anti-inflammatory assessment of Imusil

Raw 264.7 cell culture

The RAW 264.7 cells (an immortalised murine macrophage cell line) were cultured in Dulbecco's Modified Eagle's Medium high glucose medium supplemented with 10% heat-inactivated FBS and 1% penicillin/streptomycin, in an atmosphere of 5% CO_2 and 95% humidity at 37 °C. Cells were passaged after reaching 90% confluence, detached with a cell scraper, and sub-cultivated in T-75 flasks.

Cell viability assay

Raw 264.7 cells were seeded in 96-well plates at 2×10^4 cell/well and kept for overnight incubation. After the incubation, cells were separately treated with different doses of Imusil

(3.125, 6.25, 12.5, 25 and 50 µg/mL) for 1 h, followed by LPS treatment for the next 24 h. For the cell viability analysis, MTT reagent (5 mg/mL) was added to each well and incubated for 3 h. The media was removed and the formazan crystals were dissolved using DMSO. The absorbance was measured at 570 nm.

Measurement of intracellular reactive oxygen species generation

Intracellular formation of ROS was assessed using the oxidation sensitive dye DCFH-DA as a substrate (Wijesinghe et al. 2011). RAW 264.7 cells were seeded in a 24-well plate at 1×10^6 cells/well and incubated with and without 1 µg/mL of LPS and then Imusil at 25 µg/mL for 24 h. The medium was removed and cells were treated with 10 µM 2′,7′-dichlorofluorescein diacetate (DCFH-DA) for 30 min at 37 °C in the dark. The formation of dichlorofluorescin (DCF) due to oxidation of DCFH in the presence of ROS was imaged using a fluorescence microscope.

Estimation of cytokine production by ELISA technique

A total of 2×10^5 macrophages were seeded into 24-well plates and incubated overnight. Cells were treated with Imusil and then stimulated with LPS (1 µg/mL). The pro-inflammatory cytokines such as TNF-α and IL-6 concentrations were measured using ELISA kit following the manufacturer's instructions.

COX-2 enzymatic activity assay

COX-2 activity was determined by a colorimetric COX inhibitor screening assay kit according to the manufacturer's instructions. Briefly, 160 µL assay buffer and 10 µL haeme were added to the background wells, while 150 µL assay buffer, 10 µL haeme and 10 µL COX-2 enzyme were added to the 100% initial activity wells. Imusil was added to the sample wells and 10 µL DMSO was added to the background wells. The plate was carefully shaken for a few seconds and incubated for five min at 25 °C. The colorimetric substrate solution (20 µL) followed by arachidonic acid (20 µL) were added to each well. The plate was again shaken carefully for a few seconds and incubated for 5 min at 25 °C. The absorbance at 590 nm was read by a microplate reader and COX-2 enzymatic activity was calculated according to the manufacturer's instructions.

Western blotting analysis

Western blotting analysis was used to determine the protein expression. Cells were plated onto 6-well plates and pre-treated with Imusil for 1 h followed by LPS treatment and the protein extracts of RAW264.7 cells were collected using lysis buffer. The lysates were centrifuged at 15,000×*g* for 30 min at 4 °C and the supernatant containing proteins was collected. The proteins were reversed by SDS-polyacrylamide gel electrophoresis after using the Bio-Rad protein assay kit to determine the total protein concentration, then the protein bands were transferred onto polyvinylidenedifluoride (PVDF) membranes and incubated with TBST (50 mM Tris–HCl, pH 7.6, 150 mMNaCl, 0.1% Tween 20) containing 5% non-fat milk for 1 h at room temperature to block the non-specific binding sites. Following that, the PVDF membrane was incubated overnight at 4 °C with a specific primary antibody against Nox2 (1:200). After six wash cycles with TBST at 5 min intervals, membranes were incubated with HRP conjugated secondary antibody (1:1000) for 1 h at room temperature. After six wash cycles with TBST, the protein bands were stained with the enhanced chemiluminescence reagent.

Statistical analysis

Results are expressed as means and standard deviations of the control and treated cells from triplicate measurements ($n = 3$) of three different experiments. Data were subjected to one-way ANOVA and the significance of differences between means was calculated by Duncan's multiple range test, using SPSS for Windows, standard version 16 (SPSS, Inc.), and significance was accepted at $P \leq 0.05$.

Results

Characterisation of Imusil using UV–VIS spectrum, FT-IR and GC–MS analysis

UV–visible spectrum profile of Imusil

The qualitative UV–VIS spectrum profile of Imusil was selected at a wavelength from 200 to 1100 nm due to the sharpness of the peaks and proper baseline. The Imusil concentration was made as 1 mg/mL in hexane and was examined in the wavelength ranging from 200 to 1022.5 nm. The UV–VIS spectrum profile showed the peak at 201.5 nm with the maximum absorption of 0.7826 (Fig. 1).

FT-IR spectroscopic analysis

The FT-IR spectrum was used to identify the functional groups present in the given sample based on the peaks values in the region of IR radiation. When the Imusil was passed into the FT-IR, the functional groups of the components were separated based on its peaks ratio. The FT-IR spectrum profile was illustrated in Fig. 2. Six peaks at 608.67,

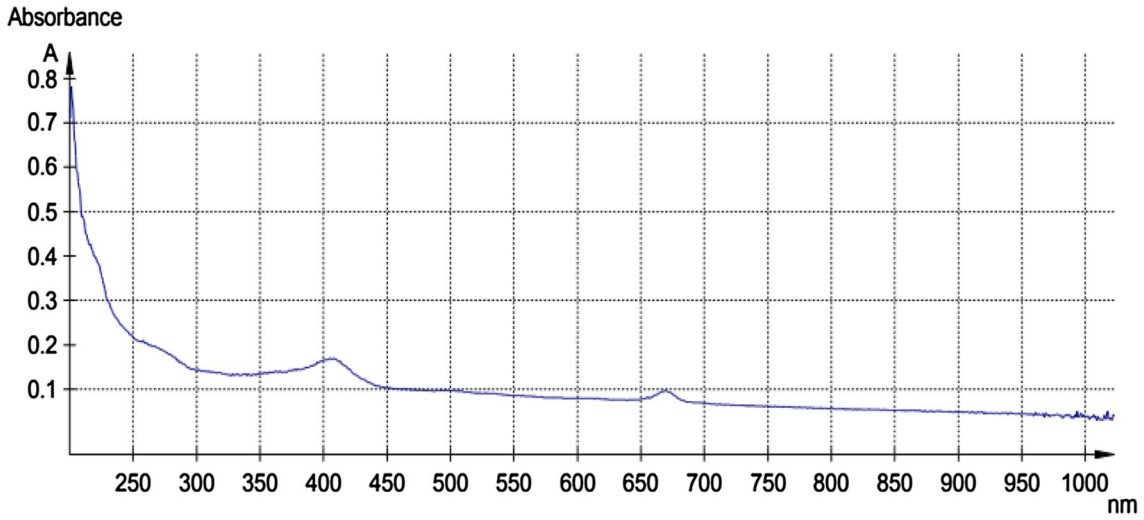

Fig. 1 UV–VIS spectrum of Imusil

1034.89, 1382.55, 1645.92, 2920.20 and 3411.12 cm^{-1} have appeared in FT-IR spectrum of Imusil. The FT-IR gave broad peak at 3411.12 cm^{-1} which indicated the presence of O–H stretching. It gave a strong peak at 1034.89 cm^{-1} which indicated the presence of C–O stretching, 608.67 cm^{-1} attributed to OH bending vibrations, the peak around 2920 cm^{-1} are due to aliphatic group, 1645.92 cm^{-1} C–O stretching, 1382.55 cm^{-1} C–O stretching vibration of carboxylic group. The FT-IR spectrum confirmed the presence of alcohols, aliphatic, carboxylic acids and esters. The results of FT-IR peak values and functional groups were represented in Table 1.

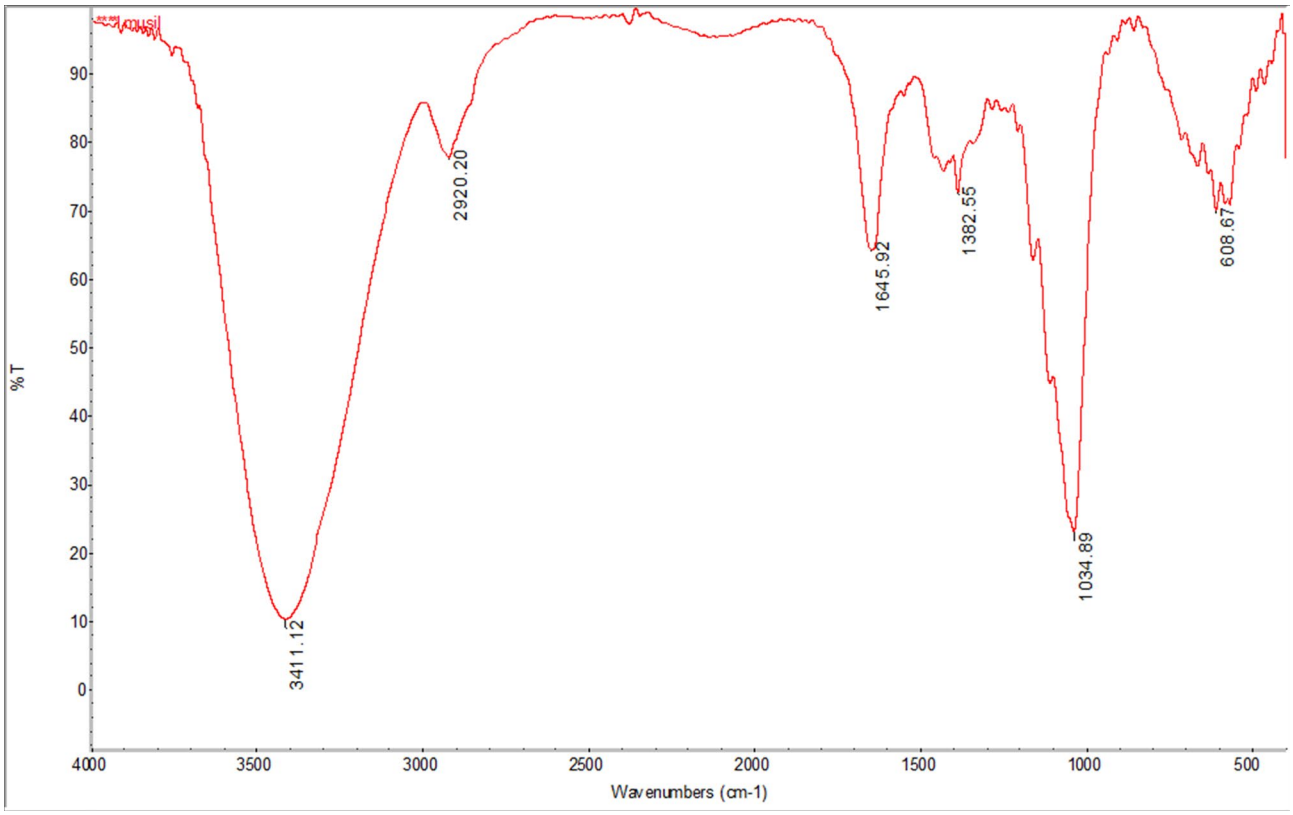

Fig. 2 FT-IR spectrum analysis of Imusil

GC–MS analysis

The chemical constituents of Imusil was identified using GC–MS analysis (Fig. 3). As elucidated by GC–MS spectrum profile, the various chemical constituents and their retention times, peak area are shown in the Table 2. The chromatogram plot of Imusil showed most prominent peaks as 3-(Octanoyloxy) propane-1,2-diyl bis(decanoate) (C_{31} H_{58} O_6) with retention time of 27.9 and peak area of 13.29%, Succinic acid, 2-methylhex-3-yl 2,2,2-trifluoroethyl ester (C_{13} H_{21} F_3 O_4) with retention time of 24.62 and peak area of 0.49%, Neophytadiene (C_{20} H_{38}) with retention time of 19.2 and peak area of 0.84%. 3,5,9-Trioxa-4-phosphaheneicosan-1-aminium, 4-hydroxy-*N*,*N*,*N*-trimethyl-10-oxo-7-[(1-oxododecyl)oxy]-, hydroxide, inner salt, 4-oxide, (R)- (C_{32} H_{64} N O_8 P) with retention time of 26.31 and peak area of 19.07%.

Maximum non-toxic dose (MNTD) and anti-viral effect of Imusil

The MNTD of Imusil was calculated with serial dilution in the Vero cell line followed by MTT assay. The MNTD of Imusil in the Vero cell line was obtained around 48.83 µg/mL after 48 h (Fig. 4). Based on this result, the obtained MNTD was used for the screening of anti-viral activity by the plaque reduction assay. Antiviral activity against SARS-CoV-2 in Vero E6 cell line through co-treatment assay at specific MNTD of Imusil shows that, it exhibited maximum viral reduction around 71% (Fig. 5), hence this data clearly indicates the promising potential and efficacy of Imusil against SARS-CoV-2 viral attack.

Investigation of cell cytotoxicity of Imusil on RAW 264.7 cells

We investigated the cytotoxic effect of Imusil followed by measuring the viability of RAW 264.7 cells using the MTT assay. In this assay, MTT is reduced by mitochondrial dehydrogenase to form a formazan product, an insoluble purple compound, and one can measure the cytotoxicity in terms of the intensity of the purple compound whereas on the other hand, dead cells do not form any purple formazan because the enzyme is degraded and lacks regular function. In the present study, the results showed that Imusil at various concentrations up to 50 µg/mL had no cytotoxic effect on RAW 264.7 cells and at the concentration of 25 µg/mL it showed 95% of cell viability as compared with the LPS treated group (Fig. 6). Based on this, 25 µg/mL was selected for the further studies. This finding revealed that Imusil ameliorated the LPS-induced cell death to retain cell viability.

Table 1 FT-IR Peak values and functional groups of Imusil

Sample	Peak value	Functional group	Vibrations
Imusil	608.67	Alcohol	OH bending
	1034.89	Alcohols, carboxylic acids and esters	C–O stretching
	1382.55	Carboxylic acid	C–O stretching
	1645.92	Carboxylic acid	C–O stretching
	2920.20	Aliphatic	CH stretching
	3411.12	Alcohol	O–H stretching

Estimation of ROS Generation using fluorescent microscopy

We examined the antioxidant potential of Imusil through its regulatory effects on free radical scavenging. In the present study, we used the DCFH-DA probe to observe whether Imusil can scavenge ROS generation inside the RAW 264.7 cells. The result revealed that there was an excessive production of ROS in LPS treated cells therefore, they produce more fluorescence. Remarkably, treatment with Imusil significantly reduced LPS-induced intracellular ROS generation and reversing almost similar to untreated cells (Fig. 7). Therefore, Imusil has the ability to control oxidative stress by inhibiting ROS generation and promoting free radical scavenging.

Imusil reduce LPS-induced Nox2/ROS activation in RAW 264.7cells

The aforementioned data suggests the radical scavenging ability of Imusil. To further confirm its protective effects against LPS-induced ROS formation, NOX-2 expression was assessed because it is linked with radical generation. As shown in Fig. 8, LPS stimulation upregulated the protein expression of NOX-2, which implies a significant increase in cellular ROS production which leads to mitochondrial damage and depletion of the antioxidant enzyme level whereas the results clearly emphasise that the Imusil attenuated Nox-2 expression, thereby maintaining the normal antioxidant pool to scavenge free radicals.

Inhibition of COX-2 signalling in LPS stimulated RAW 264.7 cells

The anti-inflammatory effect of Imusil on RAW 264.7 cells by regulating the COX-2 activity was determined as shown in Fig. 9. RAW 264.7 cells stimulated with LPS significantly increased the enzyme activity of COX-2 production as compared to normal controls. However, the supplementation of Imusil markedly reduced COX-2 activity in treated cells. These data indicate that Imusil treatment can reverse the

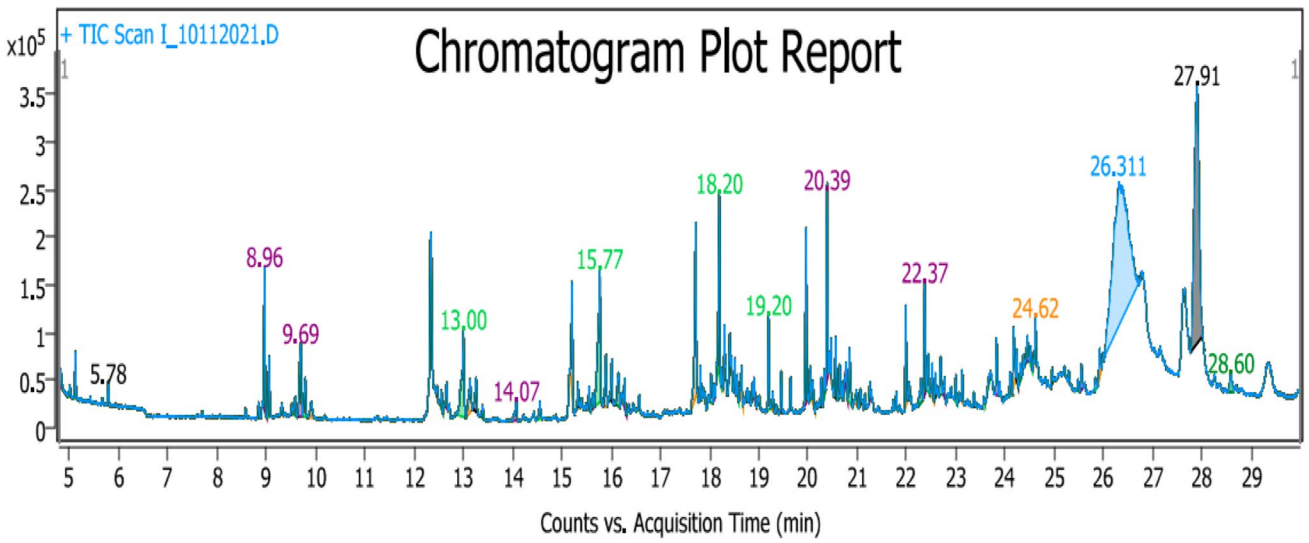

Fig. 3 GC–MS spectrum analysis of Imusil

Table 2 GC–MS Profile of Imusil. The chemical name, retention time (RT), molecular weight (MW), Molecular formula and peak area (%) of the identified compounds in Imsuil

#	Formula	Chemical names	RT	MW	Peak area (%)
1	$C_8 H_{18}$	Octane	5.78	114.141	0.18
2	$C_{12} H_{26}$	Decane, 2,4-dimethyl-	8.96	170.203	1.66
3	$C_{13} H_{28}$	Undecane, 5,7-dimethyl-	9.69	184.219	1.3
4	$C_8 H_{18}$	Hexane, 3,3-dimethyl-	13	114.141	1.66
5	$C_9 H_{16} O_2$	3,4-Hexanedione, 2,2,5-trimethyl-	14.07	156.115	0.33
6	$C_{13} H_{28}$	Undecane, 3,7-dimethyl-	15.77	184.219	2.95
7	$C_{13} H_{28}$	Undecane, 3,8-dimethyl-	18.2	184.219	3.5
8	$C_{20} H_{38}$	Neophytadiene	19.2	278.297	0.84
9	$C_{20} H_{42}$	Hexadecane, 2,6,11,15-tetramethyl-	20.39	282.329	2.27
10	$C_{13} H_{28}$	Undecane, 3,8-dimethyl-	22.37	184.219	1.31
11	$C_{15} H_{20} F_6 O_4$	Succinic acid, cyclohexylmethyl 2,2,3,4,4,4-hexafluorobutyl ester	24.62	378.127	0.49
12	$C_{32} H_{64} N O_8 P$	3,5,9-Trioxa-4-phosphaheneicosan-1-aminium, 4-hydroxy-*N*,*N*,*N*-trimethyl-10-oxo-7-[(1-oxododecyl)oxy]-, hydroxide, inner salt, 4-oxide, (R)-	26.31	621.437	19.07
13	$C_{31} H_{58} O_6$	3-(Octanoyloxy)propane-1,2-diyl bis(decanoate) –	27.9	526.423	13.29
14	$C_9 H_{16}$	1,5-Heptadiene, 2,6-dimethyl-	28.60	124.125	0.36

LPS-induced inflammatory condition via the suppression of COX-2 enzyme activity.

Inhibitory effect of Imusil on pro-inflammatory cytokines

We determined the effect of Imusil on the pro-inflammatory cytokines such as IL-6 and TNF- α in the supernatant of LPS-induced RAW 264.7 cells by ELISA technique. As shown in Fig. 10, LPS treated cells showed a significant increase in pro-inflammatory cytokine production as compared with normal control cells. Treatment of RAW 264.7 cells with a therapeutic concentration of Imusil (25 µg/mL) decreased the production of TNF-α and IL-6 thereby regulated the inflammatory condition. Hence, these results also support the potent anti-inflammatory activity of Imusil.

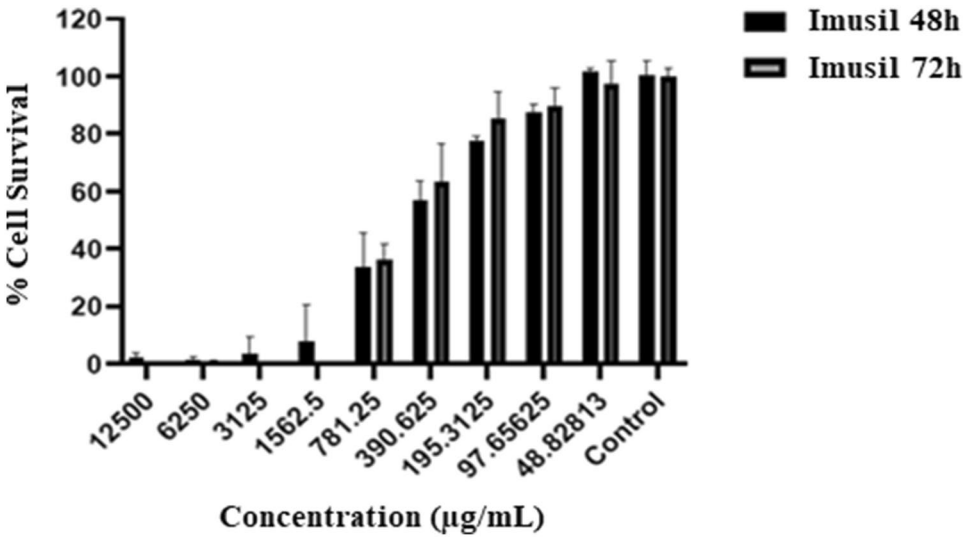

Fig. 4 MTT assay of different concentrations of Imusil on Vero E6 cell lines after 48 h and 72 h incubation. Experiments were independently repeated and data presented here represent the average of three experiments

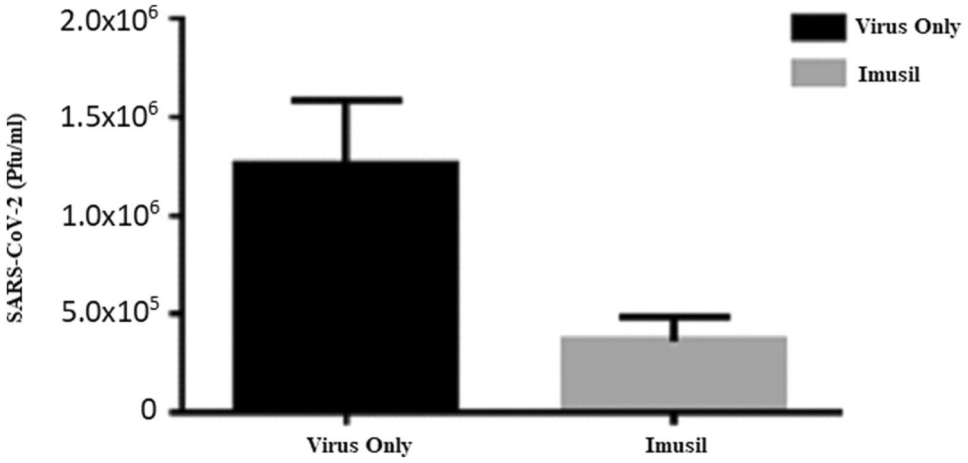

Fig. 5 Antiviral activity of Imusil against SARS-CoV-2 virus. Vero cells were treated with Imusil at MNTD. Experiments were independently repeated and data presented here represent the average of three experiments

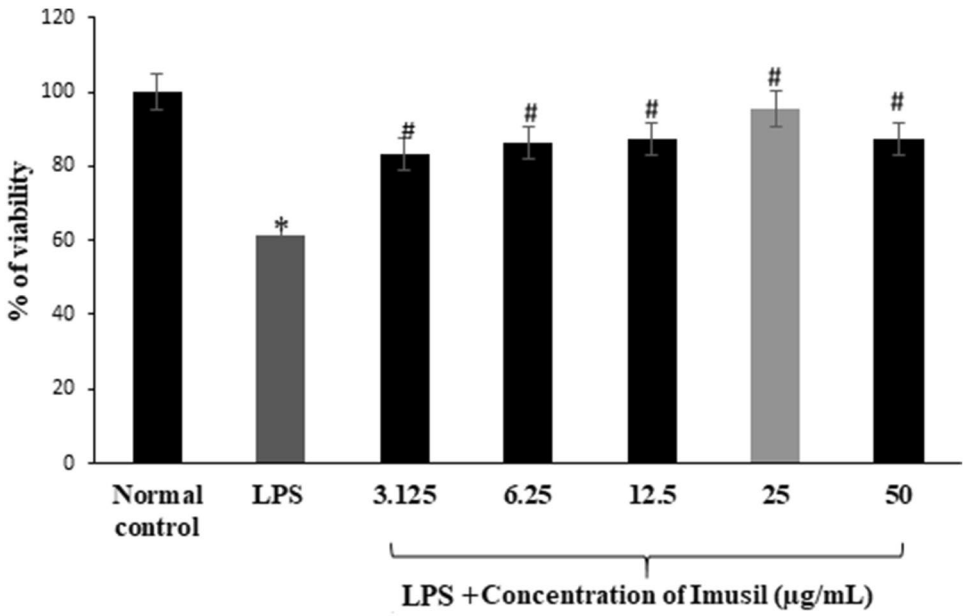

Fig. 6 Cell viability of RAW 264.7 cells with different concentrations of Imusil. *Statistical difference with Normal control, $P \leq 0.05$. #Statistical difference with LPS treated group at $P \leq 0.05$. Values are expressed as mean SD of three independent experiment

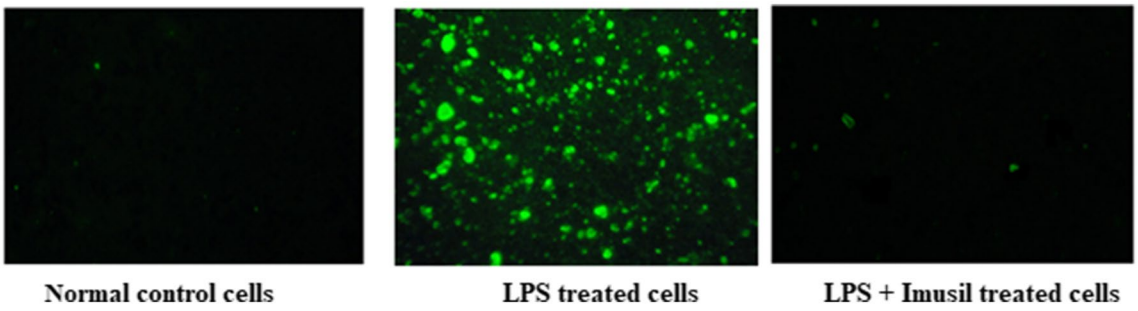

Fig. 7 Effect of Imusil on ROS production in LPS-induced RAW 264.7 macrophages by DCFHCA staining

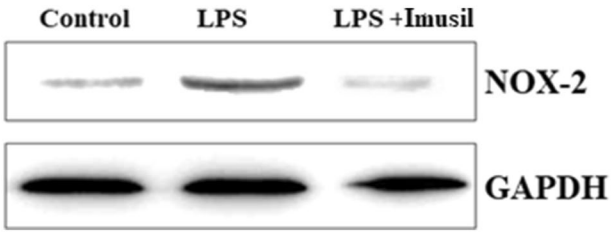

Fig. 8 Western blot analysis for the inhibitory effects of Imusil on the protein expression of NOX-2. GAPDH was used as an internal control

Discussion

Inflammation is an indispensable immune response that happens during cellular damage or when a foreign organism like virus, bacteria, fungi etc., invades the body (Ferrero-Miliani et al. 2007). Previous studies have shown that the macrophage plays a central role in regulating inflammation and immune response by triggering the release of inflammatory mediators like pro-inflammatory cytokines, COX etc. which help in the recruitment of more immune cells at the site of infection. The current scenario suggests that the prevalence of pandemics like COVID-19 or other respiratory diseases are due to the lack of prophylaxis and proper treatment measures. Recent research on herbal medicines has demonstrated their promising therapeutical properties. So, in the present study we demonstrated the anti-inflammatory and anti-viral effect of the novel polyherbal formulation Imusil.

In the present study, the investigation of Imusil revealed that various phytoconstituents such as alcohols, aliphatic, carboxylic acids, esters, diterpenes are present. Also, the GC–MS profile showed various chemical constituents such as 3-(Octanoyloxy) propane-1,2-diyl bis(decanoate), Succinic acid, 2-methylhex-3-yl 2,2,2-trifluoroethyl ester, Neophytadiene, 3,5,9-Trioxa-4-phosphaheneicosan-1-aminium, 4-hydroxy-*N*,*N*,*N*-trimethyl-10-oxo-7-[(1-oxododecyl)oxy]-, hydroxide, inner salt, 4-oxide, (R)-. Neophytadiene act as good anti-inflammatory agent and also exhibited antioxidant and cardio-protection (Bhardwaj et al. 2020).

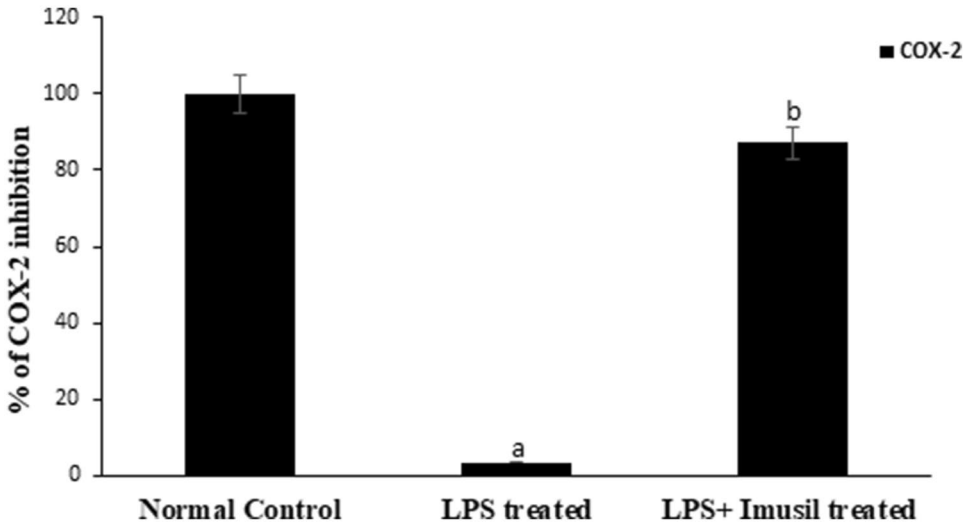

Fig. 9 Effect of Imusil in the inhibition of COX-2 activity in LPS-induced RAW 264.7 macrophages. a: Statistical difference with normal control group at $P \leq 0.05$. b: Statistical difference with LPS treated group at $P \leq 0.05$. Values are expressed as mean SD ($n = 3$)

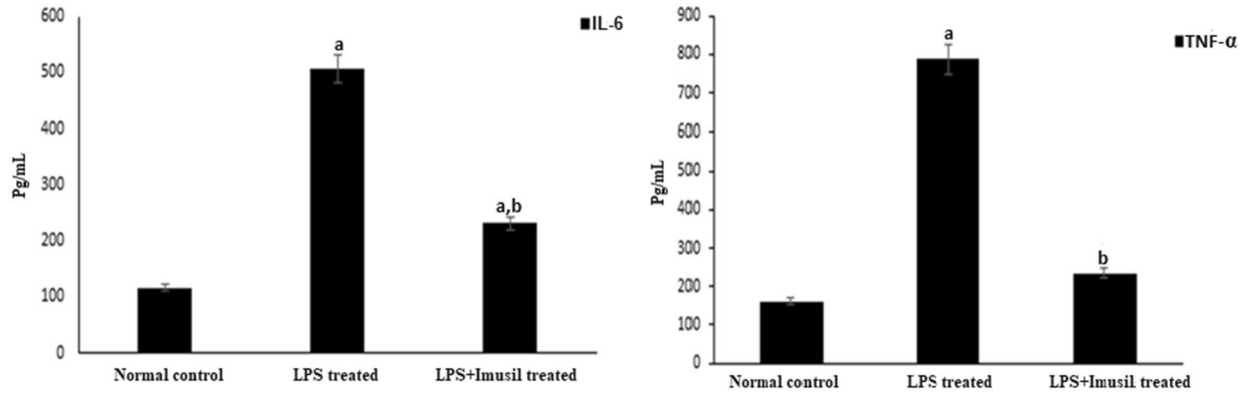

Fig. 10 Effect of Imusil on Pro-inflammatory cytokines in LPS-induced RAW 264.7 macrophages. a: Statistical difference with control group at $P \leq 0.05$. b: Statistical difference with LPS at $P \leq 0.05$. Values are expressed as mean SD ($n = 3$)

In this study, we demonstrated the potent anti-viral action of Imusil on Vero E6 kidney epithelial cells. The result of the cytotoxic assay showed that lower concentrations of Imusil increase the percentage of cell viability and the MNTD was found to be 48.83 µg/mL. That is, lower concentration is safer and non-toxic to the cells. The Imusil treatment on vero cells with the MNTD demonstrated that there was a decrease in the number of copies of the virus by 71% at 48 h. This indicates that Imusil significantly blocks viral replication and thereby reduces the number of copies of the virus. Thus, our results suggest that Imusil has virucidal effect against SARS-CoV-2 and we hypothesised that the potent anti-viral action of Imusil could be due to the various active components present in *Picrorhiza kurroa, Tinospora cordifolia* and *Emblica officinalis* which are the major ingredients of Imusil and are capable of exerting its adaptogenic activity (Panossian and Brendler 2020).

For the anti-inflammatory study, murine macrophage cells lines known as RAW 264.7 were used to assess the efficacy of Imusil to impede the inflammatory response. RAW 264.7 cells undergo a sequence of inflammatory cascades involving the activation and release of pro-inflammatory mediators and cytokines, when stimulated by LPS, a major component of the outer membrane of Gram-negative bacteria (Cuschieri and Maier 2007; Lucas and Maes 2013). The cascade of reactions may be accompanied by oxidative stress, an important target of many anti-inflammatory drugs. Use of natural herbs and plants as an alternative to anti-inflammatory drugs can inhibit their deleterious ill effects as they contain large amounts of phytochemicals which are responsible for their wide therapeutical potential (Teslim 2014). The MTT assay is a sensitive assay which is widely used to detect the cytotoxic effect of a sample. The colour development is directly proportional to the number of viable cells (Keiser et al. 2000). In the present study, various concentrations of Imusil were treated on RAW 264.7 cells to evaluate its cytotoxicity by MTT assay. The result revealed that, Imusil did not have any toxicity even at its higher doses, which shows that it is safer to use.

Oxidative stress symbolises an imbalance state between the generations of reactive oxygen species (ROS) and the cellular antioxidant defence system of the body. ROS generation plays a key role in the pathophysiology of inflammation. The ROS molecules are generated in response to diverse conditions and stimuli inside the cell, which are allied with the inflammatory process. In this study, the intracellular ROS generation was measured using the flurogenic dye DCFH-DA. LPS stimulation increased the generation of ROS in macrophage cells by activated membrane bound NADPH oxidase. But the cells treated with Imusil showed very little ROS generation as compared to LPS treated cells, which clearly shows its efficacy against ROS activity. This concludes that Imusil has the ability to act as an antioxidant to control oxidative stress by inhibiting ROS generation.

Studies have shown that the production of ROS by macrophages is mainly due to Nox-2 gene expression (Lo et al. 2013). The interconnection between NOX/ROS can be associated with immune cell response and inflammation in a variety of ways. ROS production activates the production of mitochondrial ROS (mtROS) which acts as a loop for further activation of NOX-2 (Chernyak et al. 2020), generating more ROS leads to the condition called oxidative burst, which mediates cell signalling responses (Sareila et al, 2011), and subsequently regulates a broad variety of pathological processes (Purushothaman and Sarin 2009; Pelletier et al. 2012). From the western blot analysis, it clearly shows that LPS treated RAW 264.7 cells upregulated NOX-2 protein expression and in the case of Imusil treated cells, NOX-2 protein expression was reduced to the normal level.

Emerging evidence suggest that free radical scavenging or inhibiting the expression of NOX can effectively overthrow LPS-induced cytokine production (Bonizzi et al. 1999). TNF-α and IL-6 are some of important cytokines that plays major role in the amplification inflammatory response because they are inter-dependent (Schulte et al. 2013). This cytokines in turn activates the inflammatory pathway by interacting with receptors like Toll like receptors (TLR), interleukin-6 receptors (IL-6R), TNF-α receptors and initiates mitogen activated protein kinase (MAPK), Nuclear factor kappa-B (NF-κB), Janus kinase (JAK)-signal transducer and activator of transcription (STAT) pathways (Hendrayani et al. 2016) leading to inflammation, ROS generation and thus oxidative stress. From the present study it was showed that, on LPS treated RAW 264.7 cell line produced pro-inflammatory cytokines like TNF-α and IL-6 beyond normal level, exact mechanism that happens during an immunological stress response in macrophage cells. Treatment with Imusil showed significant decline in the release of pro-inflammatory cytokines as compared with LPS stimulated macrophage cells suggesting its potent anti-inflammatory activity.

Activation of the NF-κB pathway initiates the expression of COX gene. The COX-2 enzyme is one of the two isoforms of the by-product of COX gene expression. The inducible COX-2 metabolites are involved in the induction of inflammation (Simon 1999). COX-2 mediates prostaglandin production and pain induction in the body. Imusil treatment reduced the level of COX-2 enzyme whereas LPS treated RAW 264.7 cells produced high levels of COX-2 enzyme, suggesting its potent anti-inflammatory capability.

Therefore, this study concluded that Imusil at a dose of 48.83 µg/mL of Imusil showed SARS-CoV-2 viral reduction and at 25 µg/mL showed its potent anti-inflammatory activity by reducing TNF-α, IL-6, COX-2, NOX-2, and ROS generation in RAW 264.7 murine macrophage cells. Thus, the results point outs the promising therapeutical activity of the novel polyherbal formulation of Imusil against viral and inflammatory diseases.

Acknowledgements We are gratefully acknowledge Mr. Rajesh Khatri, Managing Director of Glowderma Pvt. Ltd., Mumbai for his constant support and suggestions and also, acknowledging International Centre for Genetic Engineering and Biotechnology for providing all the facilities for conducting the anti-SARS-CoV-2 studies.

Declarations

Conflict of interest The authors declare that they have no conflict of interest. Imusil is a patent registered product (file no: TEMP/E-1/61879/2021-MUM) of Glowderma Pvt. Ltd. Mumbai, India.

References

Baer A, Kehn-Hall K (2014) Viral concentration determination through plaque assays: using traditional and novel overlay systems. J vis Exp. https://doi.org/10.3791/52065

Bhandari P, Kumar N, Singh B, Kaul VK (2008) Simultaneous determination of sugars and picrosides in picrorhiza species using ultrasonic extraction and high-performance liquid chromatography with evaporative light scattering detection. J Chromatogr A 1194:257–261. https://doi.org/10.1016/j.chroma.2008.04.062

Bhardwaj M, Sali VK, Mani S, Vasanthi HR (2020) Neophytadiene from turbinaria ornata suppresses LPS-induced inflammatory response in RAW 264.7 macrophages and sprague dawley rats. Inflammation 43(3):951–952. https://doi.org/10.1007/s10753-020-01197-x

Bonizzi G, Piette J, Schoonbroodt S et al (1999) Reactive oxygen intermediate-dependent NF-kappaB activation by interleukin-1beta requires 5-lipoxygenase or NADPH oxidase activity. Mol Cell Biol 19:1950–1960. https://doi.org/10.1128/MCB.19.3.1950

Chernyak BV, Popova EN, Prikhodko AS et al (2020) COVID-19 and oxidative stress. Biochemistry (mosc) 85:1543–1553. https://doi.org/10.1134/S0006297920120068

Chowdhury P (2020) In silico investigation of phytoconstituents from indian medicinal herb "tinospora cordifolia (giloy)" as potential inhibitors against SARS-CoV-2 (COVID-19) by molecular dynamics approach. J Biomol Struct Dyn. https://doi.org/10.1080/07391102.2020.1803968

Cuschieri J, Maier RV (2007) Oxidative stress, lipid rafts, and macrophagereprogramming. Antioxid Redox Signal 9:1485–1497. https://doi.org/10.1089/ars.2007.1670

Ferrero-Miliani L, Nielsen OH, Andersen PS, Girardin SE (2007) Chronic inflammation: importance of NOD2 and NALP3 in interleukin-1beta generation. Clin Exp Immunol 147:227–235. https://doi.org/10.1111/j.1365-2249.2006.03261.x

Forrester SJ, Booz GW, Sigmund CD et al (2018) Angiotensin II signal transduction: an update on mechanisms of physiology and pathophysiology. Physiol Rev 98:1627–1738

Garcia LF (2020) Immune response, inflammation, and the clinical spectrum of COVID-19. Front Immunol 11:4–8. https://doi.org/10.3389/fimmu.2020.01441

Griendling KK, Minieri CA, Ollerenshaw JD, Alexander RW (1994) Angiotensin II stimulates NADH and NADPH oxidase activity in cultured vascular smooth muscle cells. Circ Res 74:1141–1148. https://doi.org/10.1161/01.RES.74.6.1141

Hendrayani SF, Al-Khalaf HH, Aboussekhra A (2014x) The cytokine IL-6 reactivates breast stromal fibroblasts through transcription factor STAT3-dependent up-regulation of the RNA-binding protein AUF1. J Biol Chem 289:30962–30976

Hendrayani SF, Al-Harbi B, Al-Ansari MM, Silva G, Aboussekhra A (2016) The inflammatory/cancer-related IL-6/STAT3/NF-κB positive feedback loop includes AUF1 and maintains the active state of breast myofibroblasts. Oncotarget 7:41974–41985. https://doi.org/10.18632/oncotarget.9633

Ivanov AV, Bartosch B, Isaguliants MG (2017) Oxidative stress in infection and consequent disease. Oxid Med Cell Longev 2017:3496043

Keiser K, Johnson CC, Tipton DA (2000) Cytotoxicity of mineral trioxide aggregate using human periodontal ligament fibroblasts. J Endod 26:288–291. https://doi.org/10.1097/00004770-200005000-00010

Krupanidhi S, Abraham Peele K, Venkateswarulu TC et al (2020) Screening of phytochemical compounds of tinospora cordifolia for their inhibitory activity on SARS-CoV-2: an in silico study. J Biomol Struct Dyn. https://doi.org/10.1080/07391102.2020.1787226

Ky B, Mann DL (2020) COVID-19 clinical trials: a primer for the cardiovascular and cardio-oncology communities. JACC Basic to Transl Sci 5:501–517. https://doi.org/10.1016/j.jacbts.2020.04.003

Lampropoulou V, Sergushichev A, Bambouskova M et al (2016) Itaconate links inhibition of succinate dehydrogenase with macrophage metabolic remodeling and regulation of inflammation. Cell Metab 24:158–166. https://doi.org/10.1016/j.cmet.2016.06.004

Lo HM, Chen CL, Yang CM et al (2013) The carotenoid lutein enhances matrix metalloproteinase-9 production and phagocytosis through intracellular ROS generation and ERK1/2, p38 MAPK, and RARβ activation in murine macrophages. J Leukoc Biol 93:723–735. https://doi.org/10.1189/jlb.0512238

Lucas K, Maes M (2013) Role of the toll like receptor (TLR) radical cycle in chronic inflammation: possible treatments targeting the TLR4 pathway. Mol Neurobiol 48:190–204. https://doi.org/10.1007/s12035-013-8425-7

Mathern DR, Heeger PS (2015) Molecules great and small: the complement system. Clin J Am Soc Nephrol 10:1636–1650. https://doi.org/10.2215/CJN.06230614

Nam S-J, Oh IS, Yoon YH et al (2014) Apocynin regulates cytokine production of CD8(+) T cells. Clin Exp Med 14:261–268. https://doi.org/10.1007/s10238-013-0241-x

Panossian A, Brendler T (2020) The role of adaptogens in prophylaxis and treatment of viral respiratory infections. Pharmaceuticals (basel) 13:236. https://doi.org/10.3390/ph13090236

Park J, Min J-S, Kim B et al (2015) Mitochondrial ROS govern the LPS-induced pro-inflammatory response in microglia cells by regulating MAPK and NF-κB pathways. Neurosci Lett 584:191–196. https://doi.org/10.1016/j.neulet.2014.10.016

Pelletier M, Lepow TS, Billingham LK et al (2012) New tricks from an old dog: mitochondrial redox signaling in cellular inflammation. Semin Immunol 24:384–392. https://doi.org/10.1016/j.smim.2013.01.002

Purushothaman D, Sarin A (2009) Cytokine-dependent regulation of NADPH oxidase activity and the consequences for activated T cell homeostasis. J Exp Med 206:1515–1523. https://doi.org/10.1084/jem.20082851

Rajkumar V, Guha G, Ashok Kumar R (2011) Antioxidant and anti-neoplastic activities of picrorhiza kurroa extracts. Food Chem Toxicol 49:363–369. https://doi.org/10.1016/j.fct.2010.11.009

Sareila O, Kelkka T, Pizzolla A et al (2011) NOX2 complex-derived ROS as immune regulators. Antioxid Redox Signal 15:2197–2208. https://doi.org/10.1089/ars.2010.3635

Schulte W, Bernhagen J, Bucala R (2013) Cytokines in sepsis: potent immunoregulators and potential therapeutic targets-an updated view. Mediators Inflamm 2013:165974. https://doi.org/10.1155/2013/165974

Shwetha RJ, Tahareen S, Myrene RD (2016) Antioxidant and anti-inflammatory activity of tinospora cordifolia using in vitro models. J Chem Biol 6:497–512

Simon LS (1999) Role and regulation of cyclooxygenase-2 during inflammation. Am J Med 106:37S-42S. https://doi.org/10.1016/s0002-9343(99)00115-1

South AM, Tomlinson L, Edmonston D et al (2020) Controversies of renin-angiotensin system inhibition during the COVID-19 pandemic. Nat Rev Nephrol 16:305–307. https://doi.org/10.1038/s41581-020-0279-4

Teslim OA (2014) Side effects of non-steroidal anti-inflammatory drugs: the experience of patients with musculoskeletal disorders. Am J Heal Res 2:106. https://doi.org/10.11648/j.ajhr.20140204.11

Varga Z, Flammer AJ, Steiger P et al (2020) Endothelial cell infection and endotheliitis in COVID-19. Lancet (london, England) 395:1417–1418

Wijesinghe W, Senevirathne M, Oh MC, Jeon YJ (2011) Protective effect of methanol extract from citrus press cakes prepared by far-infrared radiation drying on H2O2-mediated oxidative damage in vero cells. Nutr Res Pract 5:389–395. https://doi.org/10.4162/nrp.2011.5.5.389

Wolff D, Nee S, Hickey NS, Michael M (2021) Risk factors for covid-19 severity and fatality: a structured literature review. Infection 49:15–28. https://doi.org/10.1007/s15010-020-01509-1